Forward-Link Soft-Handoff in CDMA With Multiple-Antenna Selection and Fast Joint Power Control

Jianming Wu, Sofiène Affes, *Member, IEEE*, and Paul Mermelstein, *Fellow, IEEE*

***Abstract*—We consider forward-link soft-handoff with multiple antenna selection and fast joint power control at high data rates in a cellular code-division multiple-access network, where signals are directed to a mobile station (MS) from antennas located at the same or different base stations. The total power transmitted to any mobile is divided among the active antennas selected according to the momentary channel conditions so as to maximize the signal-interference ratio at each MS. Multiple-antenna selection is used to mitigate the effects of both short- and long-term fading, and achieve the best soft-handoff with respect to system capacity and complexity. To achieve capacity gains with soft-handoff, we derive optimum handoff thresholds corresponding to the optimum handoff region in different cell environments. Numerical results demonstrate that under high Doppler spread and large handoff-delay conditions, the proposed soft-handoff employing two transmit antennas and the optimum handoff threshold achieves a significant gain in microcell environments, but not in macrocell environments.**

***Index Terms*—Power control, smart antennas, soft-handoff, spread spectrum multiple access, wideband code-division multiple access (CDMA).**

I. Introduction

FORWARD-LINK soft-handoff is a technique whereby a mobile station (MS) in transition between one cell and its neighbor receives the same data from both base stations (BSs) simultaneously (make before break) [1]–[5]. Such soft-handoff is employed in currently used code-division multiple-access (CDMA) systems and proposals, such as IS-95 [6] and CDMA-2000 [7]. To improve the forward-link soft-handoff performance in CDMA cellular systems, two techniques are essential: transmit diversity and fast power control. Transmit diversity is able to provide diversity benefits at a receiver when multiple transmit antennas are available. Many recent publications report on the performance of transmit diversity [8]–[10]. The performance of a number of transmit diversity schemes was examined and compared in [8] and [9], showing that if feedback from MS is permitted, selection transmit diversity (STD) can provide better performance than others such as time switched transmit diversity (TSTD) and space–time transmit diversity (STTD). However, those transmit diversities, in general, are suitable to microdiversity. Fast power control on selected antennas can provide additional benefits and reduce the effects of interference in neighboring cells in CDMA cellular systems [11], [12]. Winters [10] showed the diversity gain of transmit diversity by dividing the total transmit power equally among multiple-antennas. Heikkinen *et al.* [13] proposed an optimum power allocation scheme on the forward link, which improves performance beyond that provided by equal power transmission.

To improve the forward-link soft-handoff performance in this paper, we employ multiple-antenna selection with fast joint power control [14]. Multiple-antenna selection allows transmission of the information signal on a subset of available antennas at multiple BSs. If the antenna selection is performed across different BSs, the selection interval should be kept large to counteract long-term fading (soft-handoff), and otherwise, the selection interval should be kept small to counteract short-term fading. Therefore, this antenna selection technique can mitigate the effects of both short- and long-term fading. Note that the respective information signals are power controlled to best meet the signal-interference ratio (SIR) requirements of maximal ratio combining (MRC) reception at the MSs. This can counteract multipath fading with fast Doppler spread and reduce the received interference, particularly on the weak signal components.

The handoff-delay is the time required to execute a handoff request, including data transmission, handoff control information transmission, channel switching, and network switching [5]. This handoff-delay affects the system capacity in different cell environments. Several basic cellular structures can be considered: macrocells, microcells with line-of-sight (LOS), and microcells with nonline-of-sight (NLOS). For microcells with NLOS, the effects of handoff-delays become particularly important. In general, when an MS is moving at a high speed, handoff-delay significantly affects the system performance, possibly resulting in a high outage probability.

To mitigate the effects of handoff-delay, soft-handoff can be introduced. In currently used soft-handoff algorithms [7], [15], each MS monitors the pilot channel level received from neighboring BSs and reports to the network those pilot levels which

Manuscript received March 2, 2001; revised February 1, 2002; accepted November 22, 2002. The editor coordinating the review of this paper and approving it for publication is A. Annamalai. This work was supported in part by the Bell/Nortel/NSERC Industrial Research Chair in Personal Communications and in part by the NSERC Research Grants Program.

J. Wu is with Nortel Networks, Ottawa, ON K2H 8E9, Canada (e-mail: jianmwu@nortelnetworks.com).

S. Affes and P. Mermelstein are with INRS-Télécommunications, Université du Québec, Montréal, QC H5A 1K6, Canada (e-mail: affes@inrs-telecom.uquebec.ca; mermel@inrs-telecom.uquebec.ca).

Digital Object Identifier 10.1109/TWC.2003.811050

cross a given set of thresholds.[1] Based on the pilot information transmitted from the BS and received by the MS, the network orders the BSs to add or remove the transmission. However, this soft-handoff algorithm is performed between each MS and the serving BSs based on a fixed handoff threshold and equal power control on multiple active antennas, which results in high received interference at each MS and increases the probability of SIR outage.

The goal of this work is to analyze the soft-handoff with multiple-antenna selection and fast joint power control, and determine the optimum soft-handoff threshold, which potentially offers better performance with the practical values of handoff-delay. Under practical handoff-delay conditions, multiple-antenna selection and fast joint power control achieve the different objectives. The objective of multiple-antenna selection for soft-handoff is to mitigate the effects of both short- (due to the fast selection at the same BS) and long-term fading (due to the slow selection at the different BSs), and achieve a soft-handoff leading to higher system capacity and lower complexity. The objective of fast joint power control is to allocate the optimum transmission power to selected active antennas, which achieves a reliable connection with a sufficiently large soft-handoff region (due to the handoff-delay) and reduces the probability of SIR outage at the cell boundary.

The organization of this paper is as follows. Section II describes the system model. Section III considers the soft-handoff algorithm employing multiple-antenna selection and fast joint power control. Section IV evaluates the numerical results. Finally, Section V summarizes the paper by presenting our conclusions.

II. System Model

In this paper, we focus on a two-leg soft-handoff model which is commonly accepted for handoff analysis [16]–[18]. It can be extended to soft-handoff with three or more legs. Here, we formulate the handoff problem for the case of two BSs ($M = 2$, BS_0, and BS_1), separated by D_{total} meters, with the ith MS moving from BS_0 to BS_1 along a straight line with constant speed as shown in Fig. 1. Each BS employs J antennas ($J = 2$), and each antenna transmits data and a pilot to each MS. We assume that there are L receive antennas at each MS, and each receives P independent multipath components from each transmit antenna. We further assume that the channel response is characterized by three independent phenomena; path loss variation with distance, slow log-normal shadowing and fast multipath fading [19]. In the following sections, three path loss models for handoff discussion are considered; path loss in macrocells, microcells with LOS, and microcells with NLOS.

The channel response vector, $\underline{\mathrm{H}}_{m,j,i}(n) \in \mathbb{C}^{PL\times 1}$, corresponding to path loss, short-term fading and long-term fading between the ith MS and the jth transmit antenna at the mth BS, can be written as

$$\underline{\mathrm{H}}_{m,j,i}(n) = \left[\underline{\mathrm{H}}^T_{m,j,i,0}(n),\ \underline{\mathrm{H}}^T_{m,j,i,1}(n),\ \ldots,\ \underline{\mathrm{H}}^T_{m,j,i,L-1}(n)\right]^T \quad (1)$$

[1]The soft-handoff threshold, in recent practical systems such as 1xEV-DV [15], is assumed to be 6 dB in macrocell environments.

where $\underline{\mathrm{H}}_{m,j,i,l}(n) \in \mathbb{C}^{P\times 1}$ is represented by

$$\underline{\mathrm{H}}_{m,j,i,l}(n) = \sqrt{\mathcal{H}_{m,i}(d)} \cdot \left[\zeta_{m,j,i,l,0}(n),\ \zeta_{m,j,i,l,1}(n),\ \ldots,\ \zeta_{m,j,i,l,P-1}(n)\right]^T \quad (2)$$

and A^T is the transpose of A.

Here, $\mathcal{H}_{m,i}(d)$ is the path loss and long-term channel response between the ith MS and the mth BS, defined as

$$\mathcal{H}_{m,i}(d)_{(\mathrm{dB})} = \mathcal{L}_{m,i}(d)_{(\mathrm{dB})} + \xi_{m,i}(d)_{(\mathrm{dB})} \quad (3)$$

where $\mathcal{L}_{m,i}(d)$ and $\xi_{m,i}(d)$ represent the path loss and shadow fading measured in decibels, respectively. Finally, $\zeta_{m,j,i,l,p}(n)$ in (2) represents the short-term fading response for the pth multipath between the jth active transmit antenna at the mth BS and the lth receive antenna at the ith MS, that can be expressed in terms of inphase and quadrature components

$$\zeta_{m,j,i,l,p}(n) = \zeta^{(I)}_{m,j,i,l,p}(n) + j\zeta^{(Q)}_{m,j,i,l,p}(n). \quad (4)$$

In the handoff discussion below, for the sake of simplicity, we do not take into account the additive white Gaussian noise (AWGN). We assume that the noise only results from the multiple access interference from two BSs, due to other co-channel MSs. Also, we do not consider coding and interleaving at the transmitter and receiver.

III. Soft-Handoff With Multiple-Antenna Selection and Fast Joint Power Control

In [14], we have discussed a technique for rapid transmit antenna selection with a fast joint power control, which achieves a significant capacity gain. However, this rapid selection system is implemented under perfect selection conditions without considering the effects of handoff-delay. In fact, practical values of handoff-delay easily cause high link outage at the cell boundary between the MS and the BS due to channel variation during the handoff-delay interval. In this section, we solve this handoff-delay problem by designing a soft-handoff algorithm. We discuss soft-handoff employing multiple-antenna selection and fast joint power control in three different cell environments: macrocells, microcells with LOS, and microcells with NLOS [19]. This soft-handoff uses an optimum handoff threshold which offers the lowest probability of SIR outage. The motivation of this discussion is to show how the performance achieved by the proposed soft-handoff system under practical handoff-delay conditions can be optimized for different cell environments. The methodology discussed in this paper can be applied to other soft-handoff situations as well.

A. Available Antenna Selections

This section presents the available antenna selections which specify alternative groups of antennas on which the signals to a served MS are jointly controlled. In Fig. 1, two BSs serve each MS, and each BS and MS employs two antennas. Here, we assume that antennas A_0 and A_1 are located at BS_0, and antennas B_0 and B_1 at BS_1. With antenna selection it is possible to select one-of-four (hard-handoff), two-of-four (hard handoff or soft-handoff), and four of four (soft-handoff) active antennas.

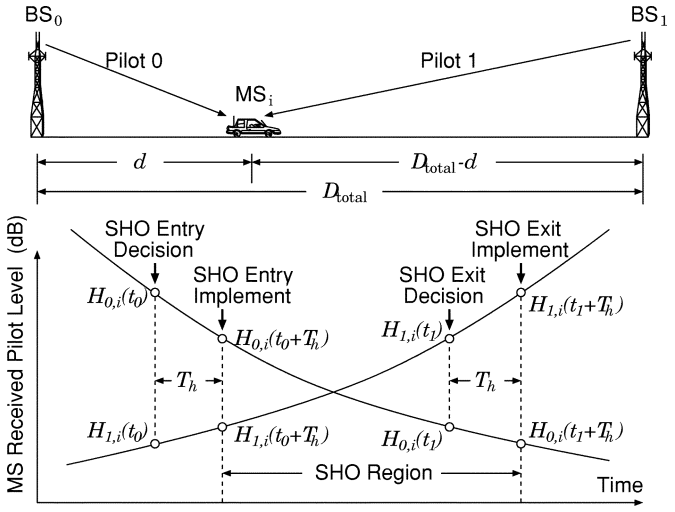

Fig. 1. System model and average received signal strength in microcell and macrocell environments.

Nevertheless, our proposed system always selects two active antennas, regardless of whether soft-handoff is or is not used. The reason for this is that use of two transmit antennas not only achieves high capacity gain, but also simplifies the implementation of soft-handoff.

Two active antennas can be selected from the same BS or different BSs. The former corresponds to no handoff, which implements slow antenna selection. Here, two active antennas are selected at every handoff-delay interval from BS_0 or BS_1. The latter corresponds to soft-handoff, which performs fast antenna selection. There, after soft-handoff decision one active antenna can be fast selected at every frame interval from the two antennas at each BS, BS_0, or BS_1.

B. Fast Joint Power Control

During an antenna selection interval the selected antennas remain unchanged and fast joint power control is employed [14]. This fast joint power control utilizes two power control factors, say $\alpha_{m,j,i}(n)$ and $\beta_i(n)$. The first factor $\alpha_{m,j,i}(n)$ is used to control power transmitted from the jth transmit antenna at the mth BS to the ith MS, as given by

$$\alpha_{m,j,i}(n) = \sqrt{\frac{\|\hat{\underline{\mathrm{H}}}_{m,j,i}(n)\|^4}{\|\hat{\underline{\mathrm{H}}}_{m,0,i}(n)\|^4 + \|\hat{\underline{\mathrm{H}}}_{m,1,i}(n)\|^4}} \tag{5}$$

where $\hat{\underline{\mathrm{H}}}_{m,j,i}(n)$ is the estimate[2] of $\underline{\mathrm{H}}_{m,j,i}(n)$ as defined in (1).

The second factor $\beta_i(n)$ is used to control transmit power for the ith MS, as given by

$$\beta_i(n) = \frac{\Lambda_i(n)}{\sum_{l=0}^{N-1} \Lambda_l(n)} \tag{6}$$

where N is the number of MSs and $\Lambda_i(n)$ is the reciprocal of received SIR for the ith MS.

[2]The standard deviation of estimation error for short-term fading $\zeta_{m,j,i,l,p}(n)$ as defined in (4) is 0.24 if 20% pilot power is taken into account [21].

The function of the two factors is quite different. The former guarantees that each MS receives sufficient power, and the latter ensures that all MSs experience the same SIR level.

In terms of fast joint power control, first, each MS transmits the control information[3] $\alpha_{m,j,i}(n)$ and $\Lambda_i(n)$ to M serving BSs through reverse dedicated channels at power control intervals (1.25 ms), which are forwarded to the mobile switching center (MSC). Then, the MSC calculates the power control factor $\beta_i(n)$ according to overall $\Lambda_i(n)$. By using $\alpha_{m,j,i}(n)$ and $\beta_i(n)$, the MSC allocates the transmission power to the jth active antenna at the mth BS for the ith MS at the ratio of $\alpha^2_{m,j,i}(n) \cdot \beta_i(n)$.

C. New Soft-Handoff Algorithm

First, let us define the difference between the channel responses received at the ith MS from two BSs corresponding to path loss and shadow fading, $\Delta_{\mathcal{H}_{0,i},\mathcal{H}_{1,i}}(d)_{(\mathrm{dB})}$, as

$$\Delta_{\mathcal{H}_{0,i},\mathcal{H}_{1,i}}(d)_{(\mathrm{dB})} = \mathcal{H}_{1,i}(d) - \mathcal{H}_{0,i}(d). \tag{7}$$

According to the definition of long-term fading $\mathcal{H}_{m,i}(d)$ as in (3) and (7) yields

$$\Delta_{\mathcal{H}_{0,i},\mathcal{H}_{1,i}}(d)_{(\mathrm{dB})} = \Delta_{\xi_{0,i},\xi_{1,i}}(d) - \Delta_{\mathcal{L}_{0,i},\mathcal{L}_{1,i}}(d) \tag{8}$$

where $\Delta_{\xi_{0,i},\xi_{1,i}}(d)$ and $\Delta_{\mathcal{L}_{0,i},\mathcal{L}_{1,i}}(d)$ are defined as

$$\Delta_{\xi_{0,i},\xi_{1,i}}(d) = \xi_{1,i}(d) - \xi_{0,i}(d) \tag{9}$$

$$\Delta_{\mathcal{L}_{0,i},\mathcal{L}_{1,i}}(d) = \mathcal{L}_{0,i}(d) - \mathcal{L}_{1,i}(d). \tag{10}$$

The difference between the channel responses received at the ith MS from two BSs, $\Delta_{\mathcal{H}_{0,i},\mathcal{H}_{1,i}}(d)$, as defined in (8), is compared with a predetermined soft-handoff threshold to make a soft-handoff decision[4] [15].

The soft-handoff state is entered or exited when the absolute value of $\Delta_{\mathcal{H}_{0,i},\mathcal{H}_{1,i}}(d)_{(\mathrm{dB})}$ is less than a predetermined soft-handoff threshold, δ_{TH} ($\delta_{\mathrm{TH}} = 0$ dB means hard handoff). We assume that the soft-handoff decision is made at every handoff-delay interval, T_h. We further assume in our discussion that two-leg soft-handoff is employed with two active transmit antennas. As mentioned before, there are two reasons for selecting two active transmit antennas. One is that two transmit antennas achieve higher capacity gain. The other is that selection with two active transmit antennas is easy to implement. The soft-handoff algorithm with multiple-antenna selection is detailed as follows.

No Handoff, if $|\Delta_{\mathcal{H}_{0,i},\mathcal{H}_{1,i}}(d)| \geq \delta_{\mathrm{TH}}$*:* The data signal is transmitted on two active antennas, both at the same BS, while the MS is traveling from distance d to $d + D_h$, where $D_h = T_h \times v$, and v is the MS velocity. In this case, two active antennas are selected either from BS_0 if $\Delta_{\mathcal{H}_{0,i},\mathcal{H}_{1,i}}(d) \leq -\delta_{\mathrm{TH}}$, or from BS_1 if $\Delta_{\mathcal{H}_{0,i},\mathcal{H}_{1,i}}(d) \geq \delta_{\mathrm{TH}}$.

Soft-Handoff, if $|\Delta_{\mathcal{H}_{0,i},\mathcal{H}_{1,i}}(d)| < \delta_{\mathrm{TH}}$*:* The data signal is transmitted on two active antennas, at different BSs, (BS_0 and BS_1), while the MS is traveling from distance d to $d + D_h$. Each active antenna can be selected from the two antennas at

[3]For the sake of simplicity, we do not consider any errors in the transmitted power control information.

[4]The use of hysteresis cannot reduce the probability of SIR outage, but avoids the ping-pong effect due to fluctuation of channel response. In this paper, we do not consider hysteresis for predetermined soft threshold. The discussion of hysteresis on soft-handoff can be found in [21].

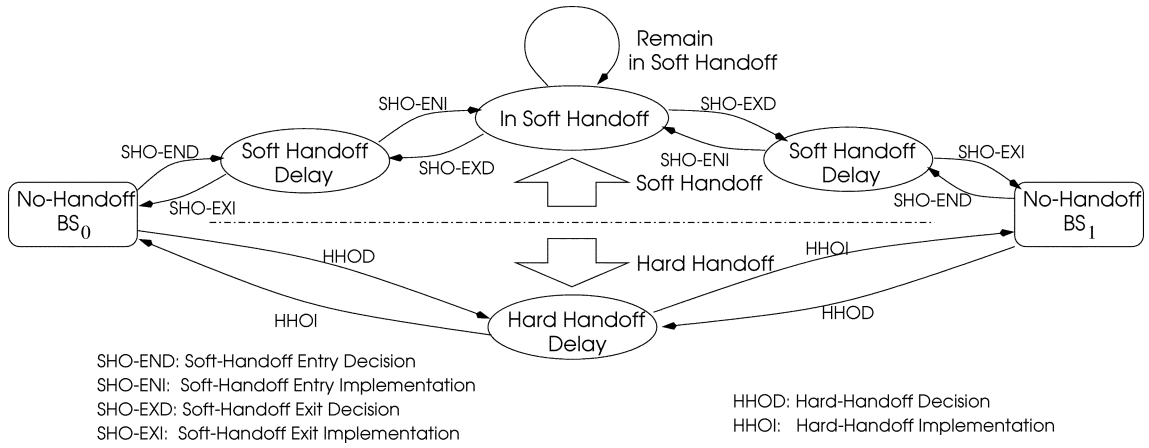

Fig. 2. The state diagram for soft-handoff and hard-handoff.

the same BS (BS_0 or BS_1) at every data frame interval, T_s, within the handoff-delay, T_h. This fast antenna selection mitigates the effect of short-term fading. The decision for this fast antenna selection is made at every data frame interval based on the channel response generated by averaging the estimate vector of $\underline{\mathrm{H}}_{m,j,i}(n)$ over the data frame interval, T_s. Generally speaking, the handoff-delay is much longer than the data frame interval, i.e., $T_h \gg T_s$. For example, the handoff-delay for Global System for Mobile Communications (GSM) is about 480 ms while the data frame is only 4.615 ms [22].

1) Objectives of Multiple-Antenna Selection: Two objectives are achieved by multiple-antenna selection. One is to determine the handoff mode at handoff-delay intervals (no handoff mode or soft-handoff mode). The other is to determine the active antenna at a BS (BS_0 or BS_1) at data frame intervals in soft-handoff mode. Handoff mode determination is made by MSC, at handoff-delay intervals T_h (slot selection). In the soft-handoff mode, one active antenna is selected from two antennas located at each BS at data frame intervals T_s (fast selection). As a result, multiple-antenna selection can mitigate the effects of both short- and long-term fading.

2) Objectives of Joint Fast Power Control: The main objective realized by fast joint power control is to allocate the optimum transmission power to the selected active antennas. In terms of soft-handoff, there exists an important additional objective. Soft-handoff, in general, has a handoff-delay problem. If the handoff-delay is large, the soft-handoff process cannot follow the rapidly changing channel, resulting in degraded system performance. Since the update rate ($1/T_{pc}$) for fast joint power control is much higher than the switching rate ($1/T_h$) for soft-handoff (i.e., $T_h \gg T_s > T_{ps}$), a reliable decision can be achieved only if the soft-handoff region is large enough. Therefore, joint fast power control is advantageous to a soft handoff system when the handoff-delay is large.

3) Implementation of Soft-Handoff: To consider the effect of handoff-delay on the soft-handoff/hard-handoff comparison, we discuss the handoff implementation with reference to the state diagram shown in Fig. 2.

Once handoff is required, the MS has to transmit the handoff control information to its desired BS through a reverse common control channel (R-CCCH). The R-CCCH uses a slotted Aloha type of mechanism (see R-CCCH in [7]). Because of possible collisions (multiple simultaneous transmissions which the BS cannot simultaneously receive), the time of retransmission should be randomized so that the retransmissions will not collide again. This process results in a variable handoff-delay[5] between handoff entry decision and handoff entry implementation.

In terms of hard handoff with a variable handoff-delay, the BS is switched and the data signal is transmitted by the selected active BS after the all BSs receive the correct handoff control information.[6] Since this process has a hard-handoff-delay between handoff entry decision and handoff entry implementation, its performance depends strongly on the value of handoff-delay.

Implementation of soft-handoff is more complex than that of hard-handoff. When soft-handoff entry is required from an MS (soft-handoff entry decision), the selected BS waits for an interval corresponding to the soft-handoff-delay and then implements the soft-handoff entry. In this soft-handoff mode, the same data signal modulated by the appropriate BS code employing the optimum joint power control is transmitted from two active antennas at two selected BSs. Coherent combining of the different signals is performed by each MS receiver. When soft-handoff exit is required from an MS (soft-handoff exit decision), the currently active BSs wait for an interval corresponding to the soft-handoff-delay, and then implement the soft-handoff exit. Outside the soft-handoff mode, the data signal modulated by the appropriate BS code employing the optimum joint power control is transmitted from two active antennas at one selected BS.

D. Analysis of Probability of SIR Outage

1) Probability of SIR Outage, $P_{\mathrm{out}}^{(n)}(d+d_n)$, Out of Soft-Handoff: Based on the probability of SIR outage as a function of $\Delta_{\mathcal{H}_{0,i},\mathcal{H}_{1,i}}(d)$, as generated in Appendix I, we derive the probability of SIR outage as a function of MS traveling distance, d. Here, we derive the result for the no-handoff state. The derivation under soft-handoff condition will be discussed in Section III-D-2.

[5]In this paper, for the sake of simplicity, we consider a handoff process with a constant handoff-delay.

[6]For the sake of simplicity, we do not consider any errors in the transmitted handoff control information.

For no-handoff as discussed in Section III-C, the following inequality holds:

$$|\mathcal{H}_{0,i}(d) - \mathcal{H}_{1,i}(d)| \geq \delta_{\mathrm{TH}}. \tag{11}$$

This inequality can be separated into two parts

$$\mathcal{H}_{0,i}(d) - \mathcal{H}_{1,i}(d) \geq \delta_{\mathrm{TH}} \quad \text{or} \quad \mathcal{H}_{0,i}(d) - \mathcal{H}_{1,i}(d) \leq -\delta_{\mathrm{TH}}. \tag{12}$$

The Case of $\mathcal{H}_{0,i}(d) - \mathcal{H}_{1,i}(d) \geq \delta_{\mathrm{TH}}$*:* In this case, according to (3), (9) and (10), $\Delta_{\xi_{0,i},\xi_{1,i}}(d)$ can be represented as

$$\Delta_{\xi_{0,i},\xi_{1,i}}(d) \leq \Delta_{\mathcal{L}_{0,i},\mathcal{L}_{1,i}}(d) - \delta_{\mathrm{TH}}. \tag{13}$$

Thus, under the condition of (13), the probability of SIR outage is given by

$$\begin{aligned} P_{\mathrm{out}}^{(n1)}(d+d_n) &= \int_{-\infty}^{\infty}\int_{-\infty}^{\Delta_{\mathcal{L}_{0,i},\mathcal{L}_{1,i}}(d)-\delta_{\mathrm{TH}}} f_{\mathrm{NHO}}\left[\Delta_{\mathcal{H}_{0,i},\mathcal{H}_{1,i}}(d+d_n)\right] \\ &\quad \cdot p\left[\Delta_{\xi_{0,i},\xi_{1,i}}(d),\, \Delta_{\xi_{0,i},\xi_{1,i}}(d+d_n)\right] \\ &\quad \cdot \mathrm{d}\Delta_{\xi_{0,i},\xi_{1,i}}(d)\mathrm{d}\Delta_{\xi_{0,i},\xi_{1,i}}(d+d_n) \end{aligned} \tag{14}$$

where $f_{\mathrm{NHO}}\left[\Delta_{\mathcal{H}_{0,i},\mathcal{H}_{1,i}}(d)\right]$ is the probability of SIR outage with respect to the parameter $\Delta_{\mathcal{H}_{0,i},\mathcal{H}_{1,i}}(d)$ in no-handoff state as generated in Appendix I, $p\left[\Delta_{\xi_{0,i},\xi_{1,i}}(d),\, \Delta_{\xi_{0,i},\xi_{1,i}}(d+d_n)\right]$ is the pdf relative to a jointly Gaussian distribution as derived in (47) of Appendix II, and d_n is the MS traveling distance with the range between $T_h v$ and $2T_h v$.

By substituting (47) into (14), the probability of SIR outage under no-handoff condition, as in (13), can be derived as

$$\begin{aligned} P_{\mathrm{out}}^{(n1)}(d+d_n) &= \frac{1}{2\sqrt{\pi}\,\sigma_\xi}\cdot\int_{-\infty}^{\infty} f_{\mathrm{NHO}}\left[\Delta_{\mathcal{H}_{0,i},\mathcal{H}_{1,i}}(d+d_n)\right] \\ &\quad \cdot \exp\left(-\frac{\Delta^2_{\xi_{0,i},\xi_{1,i}}(d+d_n)}{4\sigma_\xi^2}\right) \\ &\quad \cdot Q\left(\frac{-\Delta_{\mathcal{L}_{0,i},\mathcal{L}_{1,i}}(d)+\delta_{\mathrm{TH}}+\rho_h\Delta_{\xi_{0,i},\xi_{1,i}}(d+d_n)}{\sqrt{2(1-\rho_h^2)}\,\sigma_\xi}\right) \\ &\quad \cdot \mathrm{d}\Delta_{\xi_{0,i},\xi_{1,i}}(d+d_n) \end{aligned} \tag{15}$$

where $Q(\cdot)$ is the *Q*-function.

The Case of $\mathcal{H}_{0,i}(d) - \mathcal{H}_{1,i}(d) \leq -\delta_{\mathrm{TH}}$*:* In this case, according to (3), (9), and (10), $\Delta_{\xi_{0,i},\xi_{1,i}}(d)$ can be written as

$$\Delta_{\xi_{0,i},\xi_{1,i}}(d) \geq \Delta_{\mathcal{L}_{0,i},\mathcal{L}_{1,i}}(d) + \delta_{\mathrm{TH}}. \tag{16}$$

Thus, under the condition of (16), the probability of SIR outage is given by

$$\begin{aligned} P_{\mathrm{out}}^{(n2)}(d+d_n) &= \int_{-\infty}^{\infty}\int_{\Delta_{\mathcal{L}_{0,i},\mathcal{L}_{1,i}}(d)+\delta_{\mathrm{TH}}}^{\infty} f_{\mathrm{NHO}}\left[-\Delta_{\mathcal{H}_{0,i},\mathcal{H}_{1,i}}(d+d_n)\right] \\ &\quad \cdot p\left[\Delta_{\xi_{0,i},\xi_{1,i}}(d),\, \Delta_{\xi_{0,i},\xi_{1,i}}(d+d_n)\right] \\ &\quad \cdot \mathrm{d}\Delta_{\xi_{0,i},\xi_{1,i}}(d)\mathrm{d}\Delta_{\xi_{0,i},\xi_{1,i}}(d+d_n). \end{aligned} \tag{17}$$

By substituting (47) into (17) the probability of SIR outage under no-handoff condition, as in (16), can be derived as

$$\begin{aligned} P_{\mathrm{out}}^{(n2)}(d+d_n) &= \frac{1}{2\sqrt{\pi}\,\sigma_\xi}\cdot\int_{-\infty}^{\infty} f_{\mathrm{NHO}}\left[-\Delta_{\mathcal{H}_{0,i},\mathcal{H}_{1,i}}(d+d_n)\right] \\ &\quad \cdot \exp\left(-\frac{\Delta^2_{\xi_{0,i},\xi_{1,i}}(d+d_n)}{4\sigma_\xi^2}\right) \\ &\quad \cdot \mathrm{Q}\left(\frac{\Delta_{\mathcal{L}_{0,i},\mathcal{L}_{1,i}}(d)+\delta_{\mathrm{TH}}-\rho_h\Delta_{\xi_{0,i},\xi_{1,i}}(d+d_n)}{\sqrt{2(1-\rho_h^2)}\,\sigma_\xi}\right) \\ &\quad \cdot \mathrm{d}\Delta_{\xi_{0,i},\xi_{1,i}}(d+d_n). \end{aligned} \tag{18}$$

2) Probability of SIR Outage, $P_{\mathrm{out}}^{(s)}(d+d_n)$*, in Soft-Handoff:* In the soft-handoff state as described in Section III-C, the following inequality holds:

$$|\mathcal{H}_{1,i}(d) - \mathcal{H}_{0,i}(d)| < \delta_{\mathrm{TH}} \tag{19}$$

and thus, we may have

$$\Delta_{\mathcal{L}_{0,i},\mathcal{L}_{1,i}}(d) + \delta_{\mathrm{TH}} > \Delta_{\xi_{0,i},\xi_{1,i}}(d) > \Delta_{\mathcal{L}_{0,i},\mathcal{L}_{1,i}}(d) - \delta_{\mathrm{TH}}. \tag{20}$$

Therefore, the probability of SIR outage under the condition of (20) is given by

$$\begin{aligned} P_{\mathrm{out}}^{(s)}(d+d_n) = \int_{-\infty}^{\infty}\int_{\Delta_{\mathcal{L}_{0,i},\mathcal{L}_{1,i}}(d)-\delta_{\mathrm{TH}}}^{\Delta_{\mathcal{L}_{0,i},\mathcal{L}_{1,i}}(d)+\delta_{\mathrm{TH}}} & \\ \cdot f_{\mathrm{SHO}}\left[\Delta_{\mathcal{H}_{0,i},\mathcal{H}_{1,i}}(d+d_n)\right] & \\ \cdot p\left[\Delta_{\xi_{0,i},\xi_{1,i}}(d),\, \Delta_{\xi_{0,i},\xi_{1,i}}(d+d_n)\right] & \\ \cdot \mathrm{d}\Delta_{\xi_{0,i},\xi_{1,i}}(d)\mathrm{d}\Delta_{\xi_{0,i},\xi_{1,i}}(d+d_n) & \end{aligned} \tag{21}$$

where $f_{\mathrm{SHO}}\left[\Delta_{\mathcal{H}_{0,i},\mathcal{H}_{1,i}}(d)\right]$ is the probability of SIR outage with respect to the parameter $\Delta_{\mathcal{H}_{0,i},\mathcal{H}_{1,i}}(d)$ in soft-handoff mode as generated in Appendix I.

By substituting (47) into (21), the probability of SIR outage under the soft-handoff condition can be derived as

$$\begin{aligned} P_{\mathrm{out}}^{(s)}(d+d_n) &= \frac{1}{2\sqrt{\pi}\,\sigma_\xi}\cdot\int_{-\infty}^{\infty} f_{\mathrm{SHO}}\left[\Delta_{\mathcal{H}_{0,i},\mathcal{H}_{1,i}}(d+d_n)\right] \\ &\quad \cdot \exp\left(-\frac{\Delta^2_{\xi_{0,i},\xi_{1,i}}(d+d_n)}{4\sigma_\xi^2}\right) \\ &\quad \cdot \left[\mathrm{Q}\left(\frac{\Delta_{\mathcal{L}_{0,i},\mathcal{L}_{1,i}}(d)-\delta_{\mathrm{TH}}-\rho_h\Delta_{\xi_{0,i},\xi_{1,i}}(d+d_n)}{\sqrt{2(1-\rho_h^2)}\,\sigma_\xi}\right)\right. \\ &\quad \left. - \mathrm{Q}\left(\frac{\Delta_{\mathcal{L}_{0,i},\mathcal{L}_{1,i}}(d)+\delta_{\mathrm{TH}}-\rho_h\Delta_{\xi_{0,i},\xi_{1,i}}(d+d_n)}{\sqrt{2(1-\rho_h^2)}\,\sigma_\xi}\right)\right] \\ &\quad \cdot \mathrm{d}\Delta_{\xi_{0,i},\xi_{1,i}}(d+d_n). \end{aligned} \tag{22}$$

3) Probability of SIR Outage, $P_{\mathrm{out}}(T_h)$*, in Handoff-Delay:* The total probability of SIR outage at $(d+d_n)$, $P_{\mathrm{out}}(d+d_n)$, can be obtained by combining $P_{\mathrm{out}}^{(n1)}(d+d_n)$,

$P_{\text{out}}^{(n2)}(d+d_n)$, and $P_{\text{out}}^{(s)}(d+d_n)$, respectively, derived in (15), (18), and (22), as

$$P_{\text{out}}(d+d_n)=P_{\text{out}}^{(n1)}(d+d_n)+P_{\text{out}}^{(n2)}(d+d_n)+P_{\text{out}}^{(s)}(d+d_n). \tag{23}$$

Based on $f_{\text{SHO}}\left[\Delta_{\mathcal{H}_{0,i},\mathcal{H}_{1,i}}(d+d_n)\right]$ and $f_{\text{NHO}}\left[\Delta_{\mathcal{H}_{0,i},\mathcal{H}_{1,i}}(d+d_n)\right]$ as generated in Appendix I, we calculate $P_{\text{out}}(d+d_n)$ as defined in (23). To obtain the average probability of SIR outage as a function of handoff-delay T_h, $\overline{P}_{\text{out}}(T_h)$, we integrate the $P_{\text{out}}(d+d_n)$ in the region of $0\sim(D_{\text{total}}-D_h)$ for d and the region of $T_hv\sim 2T_hv$ for d_n, as

$$\overline{P}_{\text{out}}(T_h)=\frac{1}{T_hv\cdot(D_{\text{total}}-D_h)}\cdot\int_{T_hv}^{2T_hv}\int_{0}^{D_{\text{total}}-D_h}P_{\text{out}}(d+d_n)\,\mathrm{d}d\mathrm{d}d_n. \tag{24}$$

E. Analysis of Probability in Soft-Handoff Mode

Once the soft-handoff threshold, δ_{TH}, is determined, the probability of being in the soft-handoff mode as a function of the MS traveling distance, d, can be determined as well. The probability in soft-handoff mode is defined as the probability that the MS stays in the soft handoff mode during the soft-handoff-delay interval. We compare this probability to determine the soft-handoff region required for different cell environments.

According to the assumption of log-normal distribution of shadow fading under the soft-handoff condition as defined in (20), the probability in soft-handoff mode $P_{\text{SHO}}(d)$ can be easily determined by

$$\begin{aligned}P_{\text{SHO}}(d)&=\int_{\Delta_{\mathcal{L}_{0,i},\mathcal{L}_{1,i}}(d)-\delta_{\text{TH}}}^{\Delta_{\mathcal{L}_{0,i},\mathcal{L}_{1,i}}(d)+\delta_{\text{TH}}}p\left[\Delta_{\xi_{0,i},\xi_{1,i}}(d)\right]\mathrm{d}\Delta_{\xi_{0,i},\xi_{1,i}}(d)\\&=\mathrm{Q}\left(\frac{\Delta_{\mathcal{L}_{0,i},\mathcal{L}_{1,i}}(d)-\delta_{\text{TH}}}{\sqrt{2}\,\sigma_\xi}\right)-\mathrm{Q}\left(\frac{\Delta_{\mathcal{L}_{0,i},\mathcal{L}_{1,i}}(d)+\delta_{\text{TH}}}{\sqrt{2}\,\sigma_\xi}\right)\end{aligned} \tag{25}$$

where $p[\Delta_{\xi_{0,i},\xi_{1,i}}(d)]$ is the normal distribution, as given by

$$p\left[\Delta_{\xi_{0,i},\xi_{1,i}}(d)\right]=\frac{1}{2\sqrt{\pi}\,\sigma_\xi}\cdot\exp\left[-\frac{\Delta^2_{\xi_{0,i},\xi_{1,i}}(d)}{4\sigma_\xi^2}\right]. \tag{26}$$

IV. Numerical Results

A. Simulation Model

The network simulated consists of two cells with two BSs, each employing two antennas. Each antenna transmits data signals at a transmission rate of 115.2 kb/s, and a pilot with 20% total transmission power. The signals are spread by different PN sequences with a processing gain of 32. Each MS has two receive antennas and each receives two independent equal power multipath components. In different cell environments, the multipath fading is different; Rayleigh fading for macrocells and microcells with NLOS, and Ricean fading for microcells with LOS. A fast Doppler spread of 90 Hz is assumed. To simplify our simulations, we normalize the total transmission power from two BSs, i.e., $\mathcal{E}=1$. In order to study the probability of SIR outage, we choose a desired SIR of 5dB for its threshold. The simulation is performed with data frame lengths of 10 ms and power control intervals of 1.25 ms. Moreover, we assume that the standard deviation of short-term fading channel identification error is 0.24 [21], which will degrade the system performance with fast joint power control and fast antenna selection. We further assume that the estimation of long-term fading channel $\mathcal{H}_{1,i}(d)$ is perfect. Table I lists the numerical parameters used in the calculations.

TABLE I
Numerical Parameters Used in the Calculations for Handoff

Number of BSs, M	2
Number of antennas per BS, J	2
Number of antennas per MS, L	2
Number of multipaths per antenna, P	2
Processing gain, $\mathcal{G}$	32
Transmission rate	115.2 kbps
Threshold for SIR outage rate	5 dB
Total transmission power per cell, $\mathcal{E}$	1
Data frame intervals	10 msec
Power control intervals	1.25 msec
Standard deviation of estimation error	0.24
Doppler spread	90 Hz
Fraction of pilot trans. power, $1-\rho$	20%
PN sequence chip rate	3.6864 Mcps

In terms of the long-term shadow fading, we consider the convenient and realistic model suggested by Gudmundson [23]. Two sources of channel identification errors are considered: the time delay due to the closed loop power control, propagation and processing time, and the channel noise.

B. Path Loss Models

1) Path Loss in Macrocells: In macrocells, the following model is commonly accepted for the path loss [19], for distances ranging from 1 to 20 km, i.e.,

$$\mathcal{L}_{m,i}(d)=10\log_{10}\left(\frac{A}{d^\mu}\right) \tag{27}$$

where A is a constant, d (m) is the distance between the mth BS and the ith MS, and μ is the propagation attenuation factor.

2) Path Loss in Microcells: Two models for path loss in outdoor microcells are considered; paths traveling LOS and NLOS.

LOS: For ranges less than 500 m and antenna heights less than 20 m, some empirical measurements have shown that the received signal strength for LOS propagation along city streets can be accurately described by the two-slope model [25]–[27]

$$\mathcal{L}_{m,i}(d)=10\log_{10}\left(\frac{A}{d^\nu\left(1+\frac{d}{\mathcal{B}}\right)^\mu}\right) \tag{28}$$

where μ and ν are the propagation attenuation factors, and the parameter $\mathcal{B}$ is called the break point and ranges from 150 to 300 m.

NLOS: Grimlund and Gudmundson [28] have proposed an empirical street corner path loss model. Their model assumes LOS propagation until the MS reaches a street corner. The NLOS propagation after rounding a street corner is modeled by assuming LOS propagation from an imaginary transmitter that is located at the street corner having a transmit power equal to the received power at the street corner from the serving BS. That is, the received signal strength is given by

$$\mathcal{L}_{m,i}(d) = \begin{cases} 10\log_{10}\left(\dfrac{A}{d^{\nu}\left(1+\frac{d}{\mathcal{B}}\right)^{\mu}}\right), & d \le d_c \\ 10\log_{10}\left(\dfrac{A}{d_c^{\nu}\left(1+\frac{d_c}{\mathcal{B}}\right)^{\mu}} \cdot \dfrac{1}{(d-d_c)^{\nu}\left(1+\frac{d-d_c}{\mathcal{B}}\right)^{\mu}}\right), & d > d_c \end{cases} \tag{29}$$

where d_c (m) is the distance between the serving BS and the corner.

3) Parameters in Path-Loss Models: Based on the above path-loss models, we define the following parameters. The distance between BS_0 and BS_1 is 2000 m for macrocells and 500 m for microcells [19]. Based on the measurement results as in [23], the correlation parameter ε_D between two fading signals separated by distance D for macrocells is 0.82 with $D = 100$ m, and for microcells is 0.3 with $D = 10$ m. In addition, according to [19], the standard deviation of long-term fading σ_ξ for macrocells is 7.5 dB and for microcells is 4.3 dB. We consider only one propagation attenuation factor for macrocells, i.e., $\mu = 4$, but two factors for microcells, i.e., $\mu = 2$ and $\nu = 4$, with a break point $\mathcal{B}$ at 200 m. Finally, the distance d_c between the serving BS and the street corner for microcells with NLOS is assumed equal to the cell center, i.e., $d_c = 250$ m.

C. Evaluation—Optimum Handoff Threshold

We examine the probability of SIR outage as a function of handoff threshold δ_{TH} with two-of-four active antenna selection using (24). The objective of this calculation is to investigate the relationship between handoff-delay, cell environment, and soft handoff threshold δ_{TH}.

Fig. 3 shows the probability of SIR outage as a function of handoff threshold δ_{TH}, in macrocells, microcells with LOS, and microcells with NLOS, for various specified values of $T_h = 0.01$, 0.1, and 1.0 s. In this example, we consider the Rayleigh fading for macrocells and microcells with NLOS, Ricean fading for microcells with LOS (Rice factor of $K_R = 2$), and the MS loading of $\mathcal{C} = 15$. From the results obtained in the different cell environments, we make the following observations.

• Macrocells:

The optimum soft-handoff threshold δ_{TH} is very low, near 3 dB. Also, we find little difference in the probability of SIR outage between soft-handoff with the optimum handoff threshold and hard-handoff. Therefore, soft-handoff with the optimum soft-handoff threshold does not achieve a significant gain as opposed to hard-handoff.

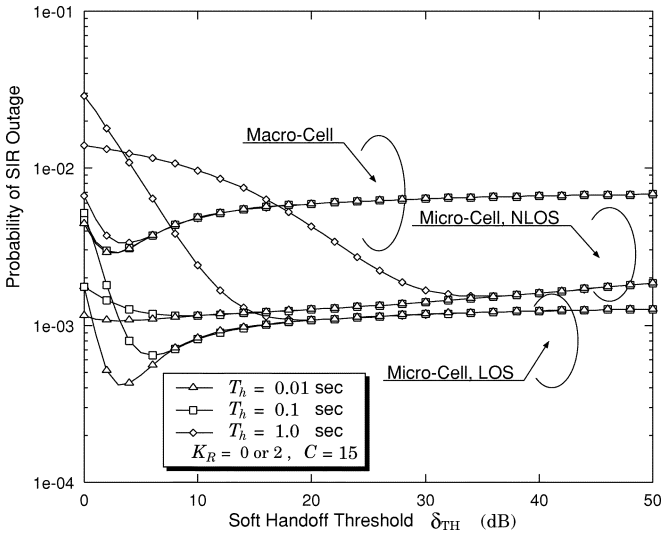

Fig. 3. Probability of SIR outage as a function of soft-handoff threshold, δ_{TH}, in macrocell (Rayleigh fading), microcell with LOS (Rice factors of $K_R = 2$), and microcell with NLOS (Rayleigh fading), for MS loading of 15, and various specified values of handoff-delay $T_h = 0.01$, 0.1, and 1.0 s.

• Microcells with LOS:

The optimum soft-handoff threshold increases with increasing handoff-delay. Introducing this threshold significantly reduces the probability of SIR outage. For example, when the handoff-delay reaches one second, the probability of SIR outage using hard-handoff is about 3×10^{-2}. This probability can be reduced to 10^{-3} using soft-handoff with the optimum soft-handoff threshold. Therefore, soft-handoff is essential under conditions of large handoff-delay.

• Microcells with NLOS:

The optimum soft-handoff threshold significantly increases with increasing handoff-delay. For example, when the handoff-delay reaches 1 s, the optimum soft-handoff threshold is about 35 dB. In this case, the soft-handoff with the optimum threshold significantly reduces the probability of SIR outage from 1.4×10^{-2} (hard-handoff) to 1.5×10^{-3}, resulting in a large capacity gain.

Table II lists the optimum threshold δ_{TH} for soft-handoff with Rayleigh fading for macrocells and microcells with NLOS, and Ricean fading (Rice factor $K_R = 2$) for microcells with LOS, for various specified values of the MS loading of 10, 15, 20, and 25. From this table, we observe that the optimum threshold δ_{TH} is dependent on handoff-delay and cell environment, but almost independent of the MS loading.

D. Evaluation—System Capacity

In the previous section, we considered soft-handoff with two-of-four active antenna selection. In this section, we first investigate the optimum number of active antennas under practical handoff-delay conditions. Second, we evaluate the system capacity by using optimum-power-control or equal-power-control. Finally, we discuss the capacity gains[7] for different soft-handoff-delays T_h at high and low Doppler spreads.

[7]The capacity gain here is defined as the gain achieved by soft handoff with an optimum soft-handoff threshold, δ_{TH}, as opposed to hard-handoff with $\delta_{\mathrm{TH}} = 0$.

TABLE II
OPTIMUM THRESHOLD δ_{TH} FOR SOFT-HANDOFF ON RAYLEIGH-FADING CHANNEL (MACROCELLS AND MICROCELLS WITH NLOS), AND RICEAN-FADING CHANNEL WITH RICE FACTORS OF $K_R = 2$ (MICROCELLS WITH LOS), FOR VARIOUS SPECIFIED VALUES OF HANDOFF-DELAY $T_h = 0.01$, 0.1, AND 1.0 S

Cell Type		Macro			LOS			NLOS		
MS Loading	T_h (sec)	0.01	0.1	1	0.01	0.1	1	0.01	0.1	1
10	δ_{TH} (dB)	3	3	4	3	6	21	3	9	37
15	δ_{TH} (dB)	3	3	4	3	6	20	3	9	35
20	δ_{TH} (dB)	2	2	3	3	5	19	3	8	33
25	δ_{TH} (dB)	2	2	3	3	5	18	3	7	31

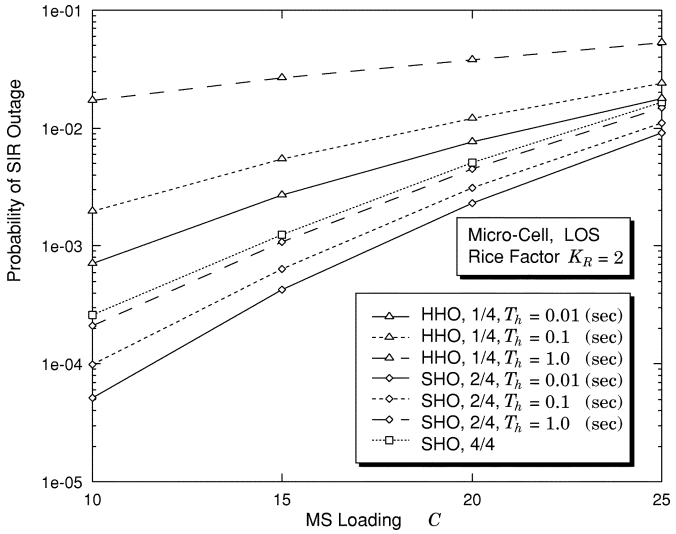

Fig. 4. System capacities for one-of-four, two-of-four, and four-of-four antenna selection in microcell with LOS (Rice factor $K_R = 2$).

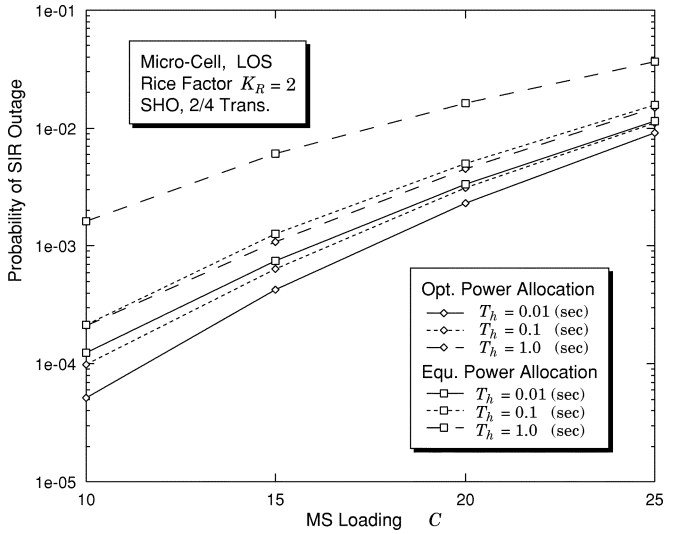

Fig. 5. System capacities for equal-power transmission and optimum-power transmission for two-of-four active antenna selection in microcell with LOS (Rice factor $K_R = 2$).

1) System Capacity for Different Antenna Selection Schemes: Fig. 4 shows an example of the probability of SIR outage as a function of system loading for one-of-four, two-of-four multiple-antenna selections, and four-of-four multiple-antenna transmission in a microcell environment with LOS. It can be seen that use of two-of-four multiple-antenna selection always outperforms one-of-four, and four-of-four, even with a large handoff-delay interval. With four-of-four multiple-antenna transmission, the system is always in handoff and capacity does not depend on the handoff-delay. With a handoff-delay of 0.1 s and an SIR outage rate limit of 5×10^{-3}, the capacity gain achieved by two-of-four multiple-antenna selection relative to four-of-four multiple-antenna transmission is 0.9 dB in microcells with LOS (1.1 dB in macrocells and 1.0 dB in microcells with NLOS). This gain grows to 2.0 dB (1.4 dB in macrocells and 1.0 dB in microcells with NLOS) compared with one-of-four multiple-antenna selection. When the handoff-delay increases (for example one second), the gain can be significant. As a consequence, with one-of-four antenna selection, only hard-handoff is available, which degrades the performance at the cell boundary. Four-of-four transmission leads to excessive channel estimation error when the MS is near one BS and far away from the other BS (because the received pilot power is very low in the latter case). Therefore, to limit the probability of SIR outage as well as reduce complexity, two-of-four active transmit antennas is the best choice for multiple-antenna selection under practical handoff conditions.

2) System Capacity for Different Fast Power Control Schemes: Fig. 5 shows an example of the probability of SIR outage as a function of system loading for two-of-four multiple-antenna selection with either optimum-power-control or equal-power-control in a microcell environment with LOS. We observe that the capacity gain[8] at an SIR outage rate of 5×10^{-3} is 0.3 dB with a handoff-delay of 0.01 s, 0.4 dB with a handoff-delay of 0.1 s, and 1.5 dB with a handoff-delay of 1 s. Thus, microcells with a large handoff-delay provide the best environment to observe the capacity benefits of optimum-power-control.

3) Capacity Gain: In Fig. 6(a), we show the optimum soft-handoff threshold δ_{TH} as a function of the handoff-delay T_h.

[8]In microcells with NLOS, the capacity gain grows to 0.4 dB with handoff-delay of 0.01 s, 0.5 dB with handoff-delay of 0.1 s, and 3 dB with handoff-delay of 1 s, while the capacity gain in macrocells is only 0.5 dB regardless of the handoff-delay, based on the analytical calculations.

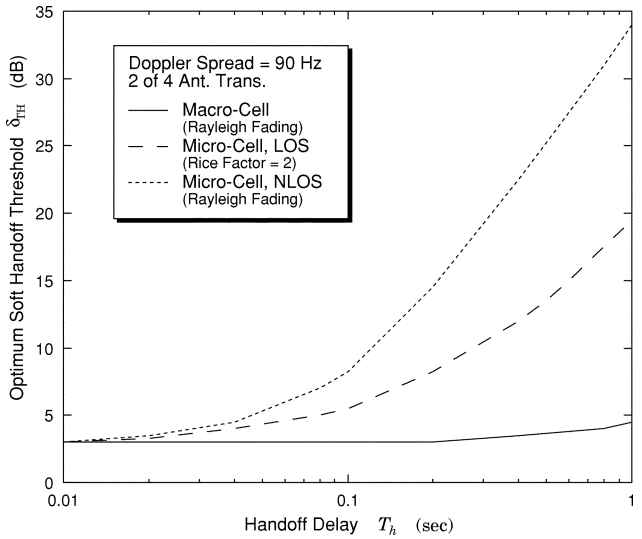

(a)

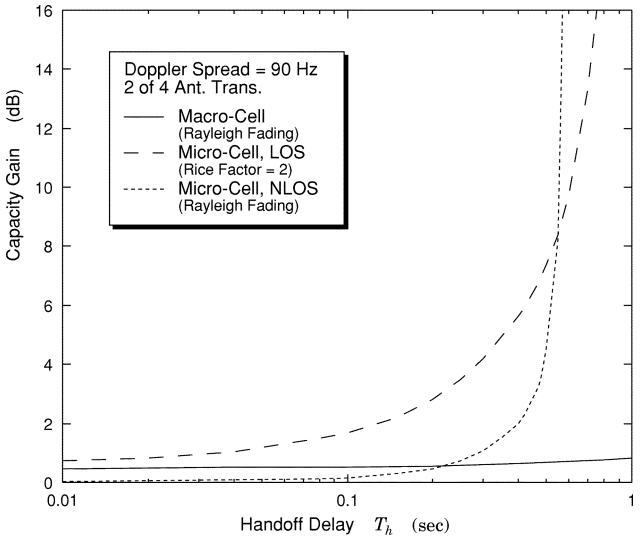

(b)

Fig. 6. (a) Optimum soft-handoff threshold δ_{TH} versus the time delay T_h. (b) Capacity gain achieved by soft-handoff as opposed to hard-handoff at an outage rate of 5×10^{-3}, and Doppler spread of 90 Hz on Rayleigh-fading channel (for macrocell and microcell with NLOS) and Ricean fading channel (for microcell with LOS).

Using these optimum thresholds, we calculate the capacity gain as a function of the handoff-delay, T_h, at an SIR outage rate of 5×10^{-3}, as shown in Fig. 6(b).

From the figures we observe that capacity gain in the macrocell environment is low (about 0.5 dB), almost independent of the handoff-delay, T_h. In the microcell environments with a low handoff-delay, soft-handoff does not achieve a significant capacity gain. As the handoff-delay increases, the capacity gain becomes high. When the handoff-delay exceeds 0.8 s, the gain increment is extremely large. The reason for this is that when the handoff-delay is over 0.8 s, hard-handoff does not achieve the required outage even with a low MS loading, resulting in a large capacity gain between soft and hard-handoff in microcells.

Also, we investigate the capacity gain at the Doppler spread of 10 Hz. We find in this case that the capacity gains are all low in the three different environments even with a large handoff-delay. When the handoff-delay T_h is one second, the capacity for macrocells is 1.4 dB, for microcells with LOS is 0.5 dB, and for microcells with NLOS is 0.2 dB. Therefore, we can say that the soft-handoff does not achieve a significant capacity gain under the low Doppler spread condition. A gain is achieved by soft-handoff only under the conditions of high Doppler spread and large handoff-delay.

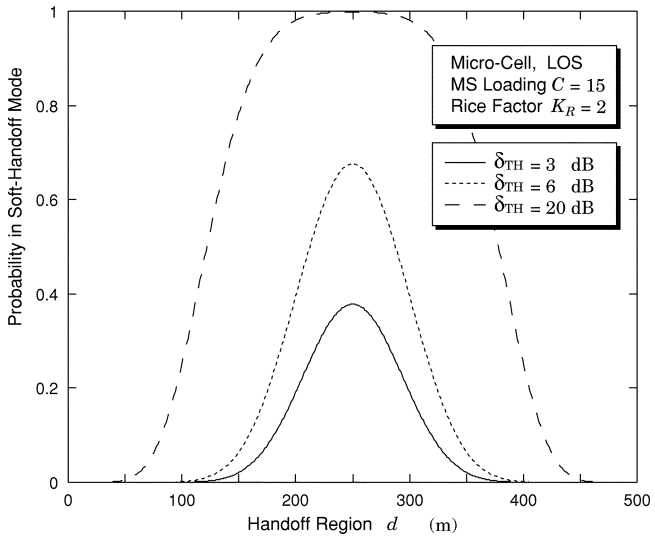

Fig. 7. Probability of being in soft-handoff mode as a function of MS traveling distance d for an MS loading of 15, and various specified values of the soft-handoff threshold in microcells with LOS (Rice factor $K_R = 2$).

E. Handoff Region

The soft-handoff algorithm employs an optimum handoff threshold which provides an optimum soft-handoff and offers the lowest probability of SIR outage. This optimum threshold, determined based on the specified handoff-delay and the cell environment, defines the soft-handoff region; if the threshold is large, the soft-handoff region becomes wide, and vice versa. This soft-handoff region can be calculated by (25), based on the predetermined optimum handoff threshold.

Fig. 7 shows the handoff region for a microcell environment with LOS. From this figure, we find that when the optimum threshold is low, the handoff region is narrow. As the threshold reaches 20 dB (corresponding to $T_h = 1$ s), the handoff region doubles in width from 200–300 to 100–400 m, where the probability in soft-handoff mode is near one at the cell boundary.

From the analytical results, we also observe that the handoff region increment in macrocells and microcells with NLOS is quite similar to that in microcell with LOS, except that macrocells show a wider region, while microcells with NLOS show a narrower region even using the same soft-handoff threshold, δ_{TH}.

V. Conclusion

We proposed a transmit antenna selection scheme with fast joint power control, whereby the same data signal is transmitted on multiple selected active antennas at multiple BSs of a CDMA network. Based on this multiple-antenna selection and fast joint power control, we have discussed the operation

of a new soft-handoff algorithm under practical conditions. Multiple-antenna selection under soft-handoff conditions can be used to mitigate the effects of both short- and long-term fading. Fast joint power control provides a reliable connection if the soft-handoff region is large enough. It ensures a sufficiently low probability of SIR outage at the cell boundary or at a street corner. To analyze the soft-handoff performance, a new methodology has been presented. This methodology is partly based on the simulation of fast joint power control and fast antenna selection, and partly based on analysis for soft-handoff with slow antenna selection. Numerical results in terms of the probability of SIR outage reveal the following.

First, in terms of multiple-antenna selection, two-of-four active transmit antennas is the best choice under practical handoff conditions. Optimum fast joint power control achieves a significant capacity gain over equal power control in microcells with long handoff-delay.

Second, with short handoff-delay, no significant benefits result from employing soft-handoff, even in the microcell environment. With a long handoff-delay at a high Doppler spread, however, soft-handoff is beneficial in microcells, but unnecessary in macrocells. As a consequence, soft-handoff achieves a significant gain in the microcell environment under the conditions of long handoff-delay and high Doppler spread, as opposed to hard-handoff. At a low Doppler spread, the capacity gains are low in all the three cell environments. Contrary to the case of high Doppler spread, the soft-handoff does not achieve a significant gain.

Third, with respect to the handoff region corresponding to the optimum soft-handoff threshold, the determination of soft-handoff threshold depends strongly upon two factors: cell environment and handoff-delay. This optimum soft-handoff threshold should be kept large so as to provide a large handoff region and result in a low probability of SIR outage at the cell boundary.

Finally, with respect to the implementation requirements, the proposed soft-handoff requires higher complexity than hard-handoff due to the processing overhead for multiple-antenna selection (macrodiversity).

Appendix I
Probability of SIR Outage With Respect to $\Delta_{\mathcal{H}_{0,i},\mathcal{H}_{1,i}}(d)$

The probability of SIR outage under the short-term fading channel condition does not lend itself to analysis, because it depends on the channel identification error calculation, the fast joint power control, and fast antenna selection at the same BS. We resort to the Monte Carlo simulation to determine it.

The contribution of this section is to offer the probabilities of SIR outage, $f_{\mathrm{NHO}}[\Delta_{\mathcal{H}_{0,i},\mathcal{H}_{1,i}}(d)]$ for no soft-handoff, and $f_{\mathrm{SHO}}[\Delta_{\mathcal{H}_{0,i},\mathcal{H}_{1,i}}(d)]$ for soft-handoff, with respect to the difference between channel responses, $\Delta_{\mathcal{H}_{0,i},\mathcal{H}_{1,i}}(d)$, based on the Monte Carlo simulation. The resulting probabilities of SIR outage will be supplied to the soft-handoff analysis. Here, we present the simulation method relative to the probability of SIR outage for both no handoff and soft-handoff, and evaluate the simulation results.

The active transmit antennas are located either on the same BS or on the different BSs. The received SIR $\Gamma_i(n)$ received at the ith MS, can be written as

$$\begin{aligned}\Gamma_i(n) &= \frac{\mathcal{E}\rho\beta_i(n-n_d)}{I_i(n)} \\ &\quad\cdot\left[\sum_{m=0}^{M-1}\sum_{j=0}^{J-1}\Re\mathrm{e}\left\{\gamma_{m,j,i}(n)\cdot\underline{\mathrm{H}}^{T}_{m,j,i}(n)\right.\right. \\ &\qquad\left.\left.\cdot\hat{\underline{\mathrm{H}}}^{*}_{m,j,i}(n)\right\}\cdot\alpha_{m,j,i}(n-n_d)\right]^2 \\ &= \frac{\mathcal{E}\rho}{\mathcal{I}_i(n)}\cdot\left[\sum_{m=0}^{M-1}\sum_{j=0}^{J-1}\sum_{l=0}^{L-1}\sum_{p=0}^{P-1}\gamma_{m,j,i}(n)\cdot\mathcal{H}_{m,i}(d)\right. \\ &\qquad\cdot\Re\mathrm{e}\left\{\zeta_{m,j,i,l,p}(n)\cdot\hat{\zeta}^{*}_{m,j,i,l,p}(n)\right\} \\ &\qquad\left.\cdot\,\alpha_{m,j,i}(n-n_d)\right]^2 \end{aligned} \tag{30}$$

where

$$\mathcal{I}_i(n) = \frac{I_i(n)}{\beta_i(n-n_d)} \tag{31}$$

and $\alpha_{m,j,i}(n)$ and $\beta_i(n)$ are the power control factors as defined in Section III-B, $\mathcal{E}$ is the total transmission power allocated to all MSs by two BSs, ρ is the fraction of total cell site power devoted to MSs ($1-\rho$ is devoted to the pilots), $\hat{\underline{\mathrm{H}}}_{m,j,i}(n)$ is the estimate of $\underline{\mathrm{H}}_{m,j,i}(n)$ as defined in (1), $\hat{\zeta}_{m,j,i,l,p}(n)$ is the estimate of $\zeta_{m,j,i,l,p}(n)$ as defined in (4), and A^T and A^* are the transpose of A and conjugate transpose of A, respectively. Another parameter we need to specify is $\gamma_{m,j,i}(n)$, which is used to indicate the active antenna. Namely, if the jth transmit antenna at the mth BS to direct to the ith MS is active, $\gamma_{m,j,i}(n)=1$, otherwise, $\gamma_{m,j,i}(n)=0$. Note that $\Re\mathrm{e}(\cdot)$ function in (30) is used to extract the real signal and reduce the interference power by one half [20].

Here, the normalized total interference power $\mathcal{I}_i(n)$ is given by

$$\begin{aligned}\mathcal{I}_i(n) &= \mathcal{E}\cdot\sum_{m=0}^{M-1}\sum_{j=0}^{J-1}\sum_{l=0}^{L-1}\sum_{p=0}^{P-1}\sum_{\tilde{m}=0}^{M-1}\sum_{\tilde{j}=0}^{J-1}\sum_{\tilde{i}=0}^{M-1}\sum_{\tilde{p}=0}^{P-1}\gamma_{\tilde{m},\tilde{j},\tilde{i}}(n) \\ &\quad\cdot\chi_{\tilde{m},\tilde{j}}(n)\cdot\left[\Re\mathrm{e}\left\{H_{\tilde{m},\tilde{j},\tilde{i},l,\tilde{p}}(n)\cdot H^{*}_{m,j,i,l,p}(n)\right\}\right]^2 \\ &= \mathcal{E}\cdot\sum_{m=0}^{M-1}\sum_{j=0}^{J-1}\sum_{l=0}^{L-1}\sum_{p=0}^{P-1}\sum_{\tilde{m}=0}^{M-1}\sum_{\tilde{j}=0}^{J-1}\sum_{\tilde{i}=0}^{M-1}\sum_{\tilde{p}=0}^{P-1}\gamma_{\tilde{m},\tilde{j},\tilde{i}}(n) \\ &\quad\cdot\gamma_{m,j,i}(n)\cdot\mathcal{H}_{\tilde{m},\tilde{i}}(d)\mathcal{H}_{m,i}(d)\chi_{\tilde{m},\tilde{j}}(n) \\ &\quad\cdot\left[\Re\mathrm{e}\left\{\zeta_{\tilde{m},\tilde{j},\tilde{i},l,\tilde{p}}(n)\cdot\hat{\zeta}^{*}_{m,j,i,l,p}(n)\right\}\right]^2 \end{aligned} \tag{32}$$

where $\chi_{m,j}(n)$ is the normalized power transmitted from the jth transmit antenna at the mth BS, as defined by

$$\chi_{m,j}(n) = \rho \cdot \sum_{i=0}^{\mathcal{C}-1} \alpha^2_{m,j,i}(n) \cdot \beta_i(n) + \frac{1-\rho}{KM} \tag{33}$$

where $\mathcal{C}$ is the MS loading, K and M are the number of active antennas ($K = 2$) and the number of BSs ($M = 2$), respectively.

If the numerator and the denominator of (30) are divided by $\mathcal{H}^2_{0,i}(d)$, the SIR, $\Gamma_i(n)$, can be represented as a function of $\Delta_{\mathcal{H}_{0,i},\mathcal{H}_{1,i}}(d)$ instead of $\mathcal{H}_{m,i}(n)$. Therefore, the equation (30) says that if $\Delta_{\mathcal{H}_{0,i},\mathcal{H}_{1,i}}(d)$ is given, the probability of SIR outage with respect to $\Delta_{\mathcal{H}_{0,i},\mathcal{H}_{1,i}}(d)$ can be determined by computer simulation.

Here, we indicate the probability of SIR outage by a function of $f_{\mathrm{NHO}}[\cdot]$ with a subscript NHO meaning "no-handoff," and by a function of $f_{\mathrm{SHO}}[\cdot]$ with a subscript SHO meaning "soft-handoff," i.e.,

$$f_{\mathrm{NHO}}[\Delta_{\mathcal{H}_{0,i},\mathcal{H}_{1,i}}(d)] = P_{\mathrm{out}}[\Delta_{\mathcal{H}_{0,i},\mathcal{H}_{1,i}}(d)], \quad \text{if } (\gamma_{0,0,i}(n) = \gamma_{0,1,i}(n) = 1 \text{ or } 0) \tag{34}$$

$$f_{\mathrm{SHO}}[\Delta_{\mathcal{H}_{0,i},\mathcal{H}_{1,i}}(d)] = P_{\mathrm{out}}[\Delta_{\mathcal{H}_{0,i},\mathcal{H}_{1,i}}(d)], \quad \text{otherwise.} \tag{35}$$

Finally, a computer simulation of (30) yields the probability of SIR outage as a function of $\Delta_{\mathcal{H}_{0,i},\mathcal{H}_{1,i}}(d)$, which is used for soft-handoff analysis. In Fig. 8(a) and (b), we show an example of the probability of SIR outage on the Rayleigh-fading channel, for one-of-four and two-of-four active antenna selection with optimum power control, and two-of-four active antenna selection with equal power control.

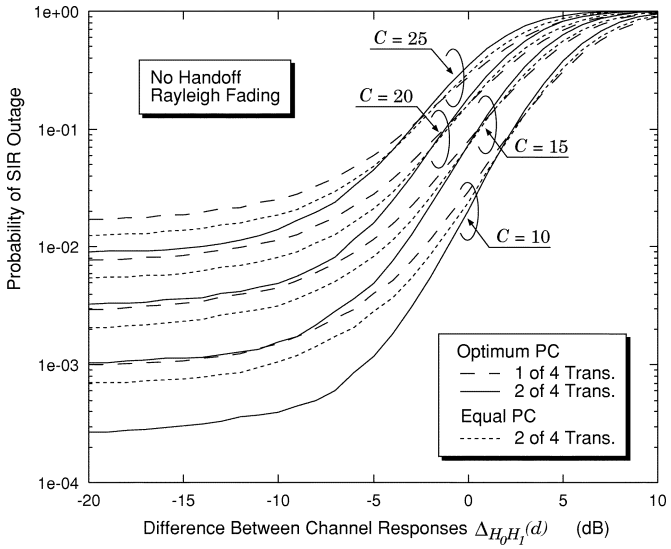

(a)

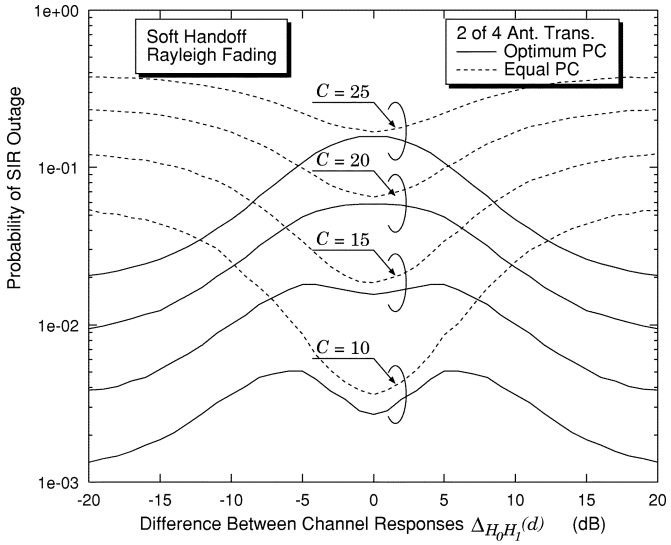

(b)

Fig. 8. Probability of SIR outage as a function of difference between channel responses, $\Delta_{\mathcal{H}_0,\mathcal{H}_1}(d)$, with (a) no handoff, and (b) soft-handoff, Rayleigh-fading channel with values of the MS loading $\mathcal{C} = 10, 15, 20$, and 25.

APPENDIX II
DERIVATION OF JOINT SHADOW FADING DISTRIBUTION $p[\Delta_{\xi_0,\xi_1}(d), \Delta_{\xi_0,\xi_1}(d+D_h)]$

Let the shadow fading levels at time t be the random variable, $\xi_i(t)_{(\mathrm{dB})}$, and at time $t + T_h$ be the random variable, $\xi_i(t + T_h)_{(\mathrm{dB})}$, where T_h is the handoff-delay interval. Here, we first prove that these two random variables are jointly Gaussian, as given by

$$p[\xi_i(t), \xi_i(t+T_h)] = \frac{1}{2\pi\sigma^2_\xi\sqrt{1-\rho^2_h}} \cdot \exp\left[-\frac{\xi^2_i(t) - 2\rho_h\xi_i(t)\xi_i(t+T_h) + \xi^2_i(t+T_h)}{2\sigma^2_\xi(1-\rho^2_h)}\right] \tag{36}$$

where σ_ξ is the standard deviation of $\xi_i(t)$, and ρ_h is the correlation coefficient between two shadow fading random variables $\xi_i(t)$ and $\xi_i(t+T_h)$ separated by time T_h, and $|\rho_h| \le 1$. Based on Gudmundsons experimental results [23], the correlation coefficient ρ_h can be represented as

$$\rho_h = \varepsilon_D^{vT_h/D} \tag{37}$$

where ε_D is the correlation between two points separated by distance D and v is the velocity of the MS (m/s). Note that $T_h = TN_h$ where T is the sampling duration and N_h is the number of samples in the handoff-delay interval.

To prove two shadow fading samples separated by time T_h to be joint Gaussian as shown in (36), let us consider the following important formula [24]

$$p[\xi(t), \xi(t+T_h)] = p[\xi(t)] \cdot p[\xi(t+T_h)|\,\xi(t)]. \tag{38}$$

Thus, instead of proving joint Gaussian distribution as in (36) directly, we need prove that $p[\xi(t)]$ and $p[\xi(t+T_h)|\xi(t)]$ are both Gaussian distribution with the probability density function (pdfs}

$$p[\xi(t)] = \frac{1}{\sqrt{2\pi}\,\sigma_\xi} \cdot \exp\left[-\frac{\xi^2(t)}{2\sigma^2_\xi}\right] \tag{39}$$

$$p\left[\xi(t+T_h)|\,\xi(t)\right] = \frac{1}{\sqrt{2\pi\sigma_\xi^2\left(1-\rho_h^2\right)}} \cdot \exp\left[-\frac{\{\xi(t+T_h)-\rho_h\xi(t)\}^2}{2\sigma_\xi^2\cdot\left(1-\rho_h^2\right)}\right]. \quad (40)$$

In terms of (39), it is naturally that the Gaussian distribution with zero mean and standard deviation of σ_ξ is recognized due to the assumption of log-normal shadow fading distribution.

In terms of (40), the Gaussian distribution is also natural due to the assumption of log-normal shadow fading. We only need to prove that this Gaussian distribution is centered at $\rho_h\xi(t)$ with standard deviation of $\sigma_\xi\sqrt{1-\rho_h^2}$, as follows.

We first show that the mean of $\xi(t+T_h)$ is centered at $\rho_h\xi(t)$. According to the generation method of shadow fading [23], we have the shadow fading samples as

$$\xi(Tk) = \rho\cdot\xi\{T(k-1)\} + (1-\rho)\cdot n\{T(k-1)\} \quad (41)$$

where $\xi(Tk)$ is the mean envelope level of shadow fading in dB that is experienced at discrete location k sampled at every T seconds, $n(Tk)$ is a zero-mean Gaussian random variable and ρ is a parameter that controls the spatial decorrelation of the shadowing.

By substituting $\xi\{T(k-1)\}, \xi\{T(k-2)\}, \ldots, \xi\{T(k-N_h+1)\}$ into (41) one after another, we obtain

$$\xi(Tk) = \rho^{N_h}\cdot\xi\{T(k-N_h)\} + \sum_{i=0}^{N_h-1}\rho^{N_h-1-i}\cdot(1-\rho)\cdot n\{T(k-N_h+i)\} \quad (42)$$

where N_h is the number of samples between $\xi(Tk)$ and $\xi\{T(k-N_h)\}$, and $TN_h = T_h$.

Since $n(Tk)$ is a while Gaussian random variable with zero mean, the mean of $\xi(Tk)$ given the event $\xi\{T(k-N_h)\}$ yields

$$E\left[\xi(Tk)\right] = \rho^{N_h}\cdot\xi\{T(k-N_h)\} = \rho_h\cdot\xi\{T(k-N_h)\} \quad (43)$$

which is equivalent to

$$E\left[\xi(t+T_h)\right] = \rho_h\xi(t) \quad (44)$$

where ρ_h is the correlation coefficient between two fading samples separated by time TN_h, as defined in (37).

Then, we show that the standard deviation of $\xi(t+T_h)$ given the event $\xi(t)$ is $\sigma_\xi\sqrt{1-\rho_h^2}$. Calculating the variance of $\xi(Tk)$ by using (42), we have

$$\begin{aligned}\mathrm{var}\left[\xi(Tk)\right] &= E\left[\left(\sum_{i=0}^{N_h-1}\rho^{N_h-1-i}\cdot(1-\rho)\cdot n\{T(k-N_h+i)\}\right)^2\right] \\ &= E\left[n^2(Tk)\right]\cdot(1-\rho)^2\cdot\sum_{i=0}^{N_h-1}\rho^{2(N_h-1-i)} \\ &= \sigma_\xi^2\cdot\left(1-\rho_h^2\right) \end{aligned} \quad (45)$$

where

$$\sigma_\xi^2 = \frac{1-\rho}{1+\rho}\cdot E\left[n^2(Tk)\right]. \quad (46)$$

Therefore, according to the mean and variance as derived in (44) and (45), the conditional Gaussian pdf of $\xi(t+T_h)$ given the event $\xi(t)$ as defined in (40) is proved for shadow fading.

Finally, according to the model of four random variables [24], the pdf with respect to $\Delta_{\xi_0,\xi_1}(d)$ and $\Delta_{\xi_0,\xi_1}(d+D_h)$, as defined in (9), can be easily derived as

$$\begin{aligned} &p\left[\Delta_{\xi_0,\xi_1}(d),\,\Delta_{\xi_0,\xi_1}(d+D_h)\right] \\ &= \int_{-\infty}^{\infty}\int_{-\infty}^{\infty} p\left[\Delta_{\xi_0,\xi_1}(d)+\xi_0(d),\,\xi_0(d),\,\Delta_{\xi_0,\xi_1}(d+D_h)\right. \\ &\quad \left.+\,\xi_0(d+D_h),\,\xi_0(d+D_h)\right]\mathrm{d}\xi_0(d)\mathrm{d}\xi_0(d+D_h) \\ &= \frac{1}{4\pi\sqrt{1-\rho_h^2}\,\sigma_\xi^2}\cdot\exp\Big[-\left\{\Delta_{\xi_0,\xi_1}^2(d)+\Delta_{\xi_0,\xi_1}^2(d+D_h)\right. \\ &\quad \left.-\,2\rho_h\Delta_{\xi_0,\xi_1}(d)\Delta_{\xi_0,\xi_1}(d+D_h)\right\}\left\{4\sigma_\xi^2\left(1-\rho_h^2\right)\right\}^{-1}\Big]. \end{aligned} \quad (47)$$

REFERENCES

[1] A. J. Viterbi, A. M. Viterbi, K. S. Gilhousen, and E. Zehavi, "Soft handoff extends CDMA cell coverage and increases reverse link capacity," *IEEE J. Select. Areas Commun.*, vol. 12, pp. 1281–1288, Oct. 1994.

[2] S. L. Su, J. Y. Yeu, and J. H. Huang, "Performance analysis of soft handoff in CDMA cellular networks," *IEEE J. Select. Areas Commun.*, vol. 14, pp. 1762–1769, Dec. 1996.

[3] C. C. Lee and R. Steele, "Effect of soft and softer handoffs on CDMA system capacity," *IEEE Trans. Veh. Technol.*, vol. 47, pp. 830–841, Aug. 1998.

[4] B. H. Cheung and V. C. M. Leung, "Network configurations for seamless support of CDMA soft handoffs between cell clusters," *IEEE J. Select. Areas Commun.*, vol. 15, pp. 1276–1288, Sept. 1997.

[5] J. Shapira, "Microcell Engineering in CDMA cellular networks," *IEEE Trans. Veh. Technol.*, vol. 43, pp. 817–825, Nov. 1994.

[6] "Mobile station-base station compatibility standard for dual-mode wideband spread spectrum cellular system," Telecommunication Industry Association, TIA/EIA/IS-95 Interim Standard, July 1993.

[7] ITU-R RTT Candidate submission, "CDMA-2000," International Telecommunications Union (ITU), TR45.5, Apr. 1998.

[8] J. S. Thompson, P. M. Grant, and B. Mulgrew, "Downlink transmit diversity schemes for CDMA networks," in *Proc. IEEE Vehicular Technology Conf.*, May 1999, pp. 1382–1386.

[9] S. Fukumoto, M. Sawahashi, and F. Adachi, "Performance comparison of forward link transmit diversity techniques for W-CDMA mobile radio," in *Proc. IEEE PIMRC'99*, Japan, Sept. 1999, pp. 1139–1143.

[10] J. H. Winters, "The diversity gain of transmit diversity in wireless systems with Rayleigh fading," *IEEE Trans. Veh. Technol.*, vol. 47, pp. 119–123, Feb. 1998.

[11] R. R. Gejji, "Forward-link-power control in CDMA cellular systems," *IEEE Trans. Veh. Technol.*, vol. 41, pp. 532–536, Nov. 1992.

[12] A. Jalali and P. Mermelstein, "Effects of diversity, power control, and bandwidth on the capacity of microcellular CDMA systems," *IEEE J. Select. Areas Commun.*, vol. 12, pp. 952–961, June 1994.

[13] T. Heikkinen and A. Hottinen, "On downlink power control and capacity with multi-antenna transmission," in *Proc. IEEE Vehicular Technology Conf.*, Canada, May 1998, pp. 475–479.

[14] J. Wu, S. Affes, and P. Mermelstein, "Transmit antenna selection with microdiversity and macrodiversity in CDMA networks," in *Proc. 20th Biennial Symp. Communications*, Queen's Univ, Kingston, ON, Canada, May 28–31, 2000, pp. 95–99.

[15] "1xEV-DV evaluation methodology—Addendum (V6),", July 25, 2001.

[16] R. Vijayan and M. Holtzman, "A model for analyzing handoff algorithms," *IEEE Trans. Veh. Technol.*, vol. 42, pp. 351–356, Aug. 1993.

[17] A. G. A. Daraiseh and M. Landolsi, "Optimized CDMA forward link power allocation during soft handoff," in *Proc. IEEE Vehicular Technology Conf.*, Canada, May 1998, pp. 1548–1552.
[18] V. V. Veeravalli and O. E. Kelly, "A locally optimal handoff algorithm for cellular communications," *IEEE Trans. Veh. Technol.*, vol. 46, pp. 603–609, Aug. 1997.
[19] G. L. Stüber, *Principles of Mobile Communications*. Norwell, MA: Kluwer, 1996.
[20] S. Affes and P. Mermelstein, "A new receiver structure for asynchronous CDMA: STAR—The spatio-temporal array-receiver," *IEEE J. Select. Areas Commun.*, vol. 16, pp. 1411–1422, Oct. 1998.
[21] J. Wu, "Soft handoff using multiple antenna selection for CDMA cellular systems," Ph.D. dissertation, INRS Telecommunications, Dec. 2000.
[22] T. S. Rappaport, *Wireless Communications: Principles Practice*. Piscataway, NJ: IEEE, 1996.
[23] M. Gudmundson, "Correlation model for shadow fading in mobile radio systems," *Electron. Lett.*, vol. 27, pp. 2145–2146, Nov. 1991.
[24] H. Stark and J. W. Woods, *Probability, Random Processes, and Estimation Theory for Engineers*. Englewood Cliffs, NJ: Prentice-Hall, 1994.
[25] W. C. Jakes, Jr., *Microwave Mobile Communications*. New York: Wiley, 1974.
[26] M. Hata and T. Nagatsu, "Mobile location using signal strength measurements in cellular systems," *IEEE Trans. Veh. Technol.*, vol. 29, pp. 245–251, 1980.
[27] A. Rustako, N. Amitay, G. Owens, and R. Roman, "Radio propagation at microwave frequencies for line-of-sight microcellular mobile and personal communications," *IEEE Trans. Veh. Technol.*, vol. 40, pp. 203–210, Feb. 1991.
[28] O. Grimlund and B. Gudmundson, "Handoff strategies in microcellular systems," in *Proc. IEEE Vehicular Technology Conf.*, St. Louis, MO, May 1991, pp. 505–510.

Jianming Wu received the M.S. degree in electrical and computer engineering from Yokohama National University, Japan, in 1996, and the Ph.D. degree in telecommunications from INRS, Quebec University, Canada, in 2001.

From 1996 to 1997, he was a system engineering designer at Fuji-soft, Japan, where he was involved in algorithm design for the PHS system. From 1997 to 1998, he was a Research Assistant with Nortel Networks, Ottawa, ON, Canada, working on Rake receiver for IS-95. Since 2001, he has been with the Wireless Technology Labs (WTL), Nortel Networks, as a System Engineer. His research interests are in aspects of antenna arrays and CDMA for wireless communication systems.

Sofiène Affes (S'94–M'95) received the Diplôme d'Ingénieur in electrical engineering in 1992 and the Ph.D. degree with honors in signal and image processing in 1995, both from the École Nationale Supérieure des Télécommunications, Paris, France.

He has been with INRS-Telecommunications, University of Quebec, Montreal, Canada, as a Research Associate from 1995 to 1997, then as an Assistant Professor until 2000. Currently, he is an Associate Professor in the Personal Communications Group. His research interests are in statistical signal and array processing, synchronization, and multiuser detection in wireless communications. Previously, he was involved in the European ESPRIT projects 2101 ARS on speech recognition in adverse environments in 1991, and 6166 FREETEL on hands-free telephony, from 1993 to 1994. In 1997, he participated in the major program in personal and mobile communications of the Canadian Institute for Telecommunications Research, Montreal, QC, Canada. Since 1998, he has been leading the radio design and signal processing activities of the Bell/Nortel/NSERC Industrial Research Chair in Personal Communications at INRS-Telecommunications. In March 2003, he has been granted a Canada Research Chair in High-Speed Wireless Communications.

Prof. Affes is the corecipient of the 2002 Prize for Research Excellence of INRS.

Paul Mermelstein (S'58–M'63–SM'77–F'94) received the B.Eng. degree in engineering physics from McGill University, Montreal, Canada, in 1959, and the S.M., E.E., and D.Sc. degrees in electrical engineering from the Massachusetts Institute of Technology, Cambridge, MA, in 1960, 1963, and 1964, respectively.

From 1964 to 1973, he was a Member of the Technical Staff in the Speech and Communications Research Department, Bell Laboratories, Murray Hill, NJ. From 1973 to 1977, he was a Member of the Research Staff at Haskins Laboratories, New Haven, CT, conducting research in speech analysis, perception, and recognition. From 1977 to 1994, he was with Bell Northern Research, in a variety of management positions leading research and development activities in speech recognition, speech coding, and personal communications. From 1994 to 2000, he was the Leader of the major program in personal and mobile communications of the Canadian Institute for Telecommunications Research, Montreal, QC, Canada. He is a past Associate Editor for Speech Processing of the *Journal of the Acoustical Society of America*.

Dr. Mermelstein is an Editor for Speech Communications of The IEEE TRANSACTIONS ON COMMUNICATIONS. He holds the Bell/Nortel/NSERC Industrial Research Chair in Personal Communications at INRS-Telecommunications, University of Quebec, Montreal, Canada. He is the corecipient of the 2002 Prize for Research Excellence of INRS.